Multi-scale surveillance reveals substantial egg-laying winter activity in *Aedes albopictus* mosquito populations across temperate Europe

Daniele Da Re[1,*], Giovanni Marini[1], Alessandro Albieri[2], Paola Angelini[3], Karin Bakran-Lebl[4], Beniamino Caputo[5], Marco Carrieri[2], Maria Liliana Di Pasquale[9], Claudio De Liberato[6], Sarah Droghei[6,7,1], Irene Del Lesto[7], Alessandra Franceschini[8], Chiara Gentile[5], Peter Hufnagl[4], Guillaume Lacour[9], Valeria Lencioni[8], Francesco La Russa[10], Riccardo Paolo Lia[11], Eleonora Longo[12], Mateusz Markowicz[4], Bruno Mathieu[13], Antoine Mignotte[9], Bianca Modespacher[14,15], Pie Müller[14,15], Francesca Paoli[8], Alessia Ricci[11], Federico Romiti[7], Barbara Seebacher[4], Rodolfo Veronesi[2], Roberto Rosà[12,**], Annapaola Rizzoli[1,**]

[1] Research and Innovation Centre, Fondazione Edmund Mach, Italy

[2] Centro Agricoltura Ambiente “G. Nicoli” (CAA), Italy

[3] Regione Emilia-Romagna, Italy

[4] AGES – Austrian Agency for Health and Food Safety, Austria

[5] Dipartimento di Sanità Pubblica e Malattie Infettive, Università La Sapienza di Roma, Italy

[6] Università della Tuscia, Italy

[7] Istituto Zooprofilattico Sperimentale del Lazio e della Toscana "M. Aleandri", Italy

8 MUSE – Museo delle Scienze di Trento, Italy

9 Altopictus, Pérols, France

10 Istituto Zooprofilattico Sperimentale della Sicilia "A. Mirri", Italy

[1]1 Università di Bari, Italy

[1]2 Università di Trento, Italy

[1]3 Institute of Bacteriology and Parasitology, UR3073 PHAVI, University of Strasbourg, France

[1]4 Swiss Tropical and Public Health Institute, Kreuzsstrasse 2, 4123 Allschwil, Switzerland

[15] University of Basel, Petersplatz 1, 4001 Basel, Switzerland

*corresponding author: daniele.dare@fmach.it

**shared last co-authorship

Author Contributions

Conceptualisation: Daniele Da Re and Roberto Rosà conceived the initial idea for the study, with relevant contributions from all the co-authors.
Sampling protocol design: All authors jointly discussed, refined, and agreed upon the sampling protocol.
Field sampling: Alessandro Albieri, Karin Bakran-Lebl, Beniamino Caputo, Marco Carrieri, Maria Liliana Di Pasquale, Sarah Droghei, Irene del Lesto, Alessandra Franceschini, Chiara Gentile, Peter Hufnagl, Guillaume Lacour, Valeria Lencioni, Francesco La Russa, Riccardo Paolo Lia, Mateusz Markowicz, Bruno Mathieu, Antoine Mignotte, Bianca Modespacher, Pie Müller, Francesca Paoli, Alessia Ricci, Federico Romiti, Barbara Seebacher, and Rodolfo Veronesi performed the field sampling across all monitoring sites.
Data analysis: Daniele Da Re analysed the data, with substantial contributions from Giovanni Marini and Roberto Rosà. Eleonora Longo performed the Citizens Science observations data gathering and analysis.
Writing: Daniele Da Re led the writing of the first manuscript draft. All authors contributed critically to the development, revision, and final approval of the manuscript.

Acknowledgments

The contents of this publication are the sole responsibility of the authors and do not necessarily reflect the views of the European Commission.
KBL, MM, PH, BS wish to thank the City of Graz (Austria) for the support during the winter sampling activities. GL and AM would also like to thank all Altopictus technical staff who contributed to this work (Flavien Thiers, Jeanne Hanin, Hugo Peyret, Alix Enjolras, Arnaud Jacqueton, Guillaume Boisramé, Aurélie Dupeyron).

Declaration of interests

All authors report no conflicts of interest.

Declaration of generative AI use

During the preparation of this work, Daniele Da Re used Claude Sonnet 4.6 to check the grammatical consistency and flow of the text of the first draft. After using this tool, all the authors reviewed and edited the content as needed and took full responsibility for the content of the published article.

Summary

Background

The Asian tiger mosquito (*Aedes albopictus*), a competent vector for dengue, chikungunya, and Zika viruses, has expanded rapidly across temperate Europe. European vector surveillance typically operates May to October, assuming winter diapause precludes activity and transmission risk. However, recent field observations suggest sustained egg-laying winter activity in southern European populations, potentially extending arbovirus transmission risk. We aimed to quantify winter ovitrap activity patterns across temperate Europe and assess their implications for mosquito surveillance across temperate Europe.

Methods

In this multi-scale observational study, we deployed standardised ovitraps from October 2024 to May 2025 across 12 locations spanning 35–48°N (Italy, France, Switzerland, Austria; n=345 trap-weeks), complemented by 14-year longitudinal surveillance (2011–2025) from Emilia-Romagna, northern Italy (n=1999 trap-weeks across 10 municipalities). We used binomial generalised additive models to quantify the effects of photoperiod, temperature, and precipitation on ovitrap positivity while accounting for spatial heterogeneity. We calculated trap effort requirements for reliable winter detection and assessed temporal trends in spring versus autumn activity.

Findings

Winter ovitrap positivity was common and geographically structured. Photoperiod was the dominant driver ($p<0.001$), with southern Mediterranean sites maintaining detection probabilities >20% throughout December–January, while northern sites showed near-complete cessation. Temperature significantly modulated activity with reduced detection below 10°C. Substantial spatial heterogeneity persisted, indicating that local factors override climate variables. Spring positivity (January–May) was 73% lower than autumn (October–December; $p<2\times10^{-11}$), reflecting overwintering population bottlenecks. Fourteen-year regional trends showed no significant autumn increase, but a modest spring increase, though confounded by temperature and potential surveillance artefacts. Power analysis revealed current surveillance (median 10 traps per site-week) substantially exceeds autumn requirements (4 traps for 80% detection) but falls short for spring (13 traps required).

Interpretation

Ovipositing winter activity of *Ae. albopictus* in temperate Europe is widespread and structured by photoperiod and geography rather than being rare or negligible. Current May-October surveillance paradigms miss substantial autumn activity and likely underestimate population persistence capacity. Persistent egg-laying winter activity in Mediterranean climates, though homodynamicity was not detected, combined with recent evidence of lower-than-expected thermal transmission thresholds, suggests that arbovirus risk assessment should consider extended seasonal windows or better be estimated at an annual time frame. While our results demonstrate that winter monitoring is essential to uncover ecological patterns, multi-year continental surveys are required to confirm patterns and disentangle the drivers of seasonal

variability. These results provide a foundation for adaptive surveillance strategies as *Ae. albopictus* continues expanding into increasingly temperate regions under climate change.

Funding

Daniele Da Re was supported by the Marie Sklodowska-Curie Actions - Postdoctoral fellowship Nr. 101106664. GL and AM were supported through Altopictus internal resources. BC and CG were supportted by the NextGenerationEUMUR PNRR Extended Partnership initiative on Emerging Infectious Diseases (Project no. PE00000007, INF-ACT). AR was partially funded by the Autonomous Province of Trento under the grant " One Health epidemiological surveillance".

Keywords: Asian tiger mosquito, diapause, photoperiod, climate change, phenology, winter surveillance

1. Introduction

Aedes albopictus (Skuse, 1895), commonly known as the Asian tiger mosquito, has emerged as a major medical and veterinary health concern across temperate regions due to its role as a competent vector for a number of pathogens, such as arboviruses and nematodes [1,2]. Since its first detection in Europe in 1979 [3], *Ae. albopictus* has expanded its distributional range rapidly northward, and now it is established in many countries across the continent [4]. This expansion has coincided with increasing autochthonous pathogens transmission in previously non-endemic areas, as in the case of dengue and chikungunya outbreaks in Mediterranean Europe [5,6].

The public health significance of these outbreaks extends beyond mortality. Even small, late-season transmission events generate substantial morbidity and economic burden in local populations, especially for those with limited vector control infrastructure [7]. Recent evidence that chikungunya can be transmitted at temperatures as low as 13.8°C [8], well within autumn and spring temperatures across Mediterranean Europe, challenges the assumption that transmission risk is limited to summer months only [9]. Combined with extended mosquito longevity at moderate temperatures [10], this suggests near year-round arbovirus risk in southern European climates [11].

Nevertheless, in temperate climates *Ae. albopictus* populations have historically been assumed to undergo obligate photoperiodic diapause during autumn, with dormant eggs overwintering in arrested development [12,13]. This paradigm has shaped surveillance strategies across Europe, where monitoring programs typically operate May-October, assuming egg-laying winter activity is negligible [14]. However, accumulating field observations from southern Europe, specifically Spain, Italy and Greece, challenge this view [11,15,16], reporting winter egg detections. Whether these findings represent continuous breeding versus opportunistic hatching during mild periods remains unclear.

It follows that several phenological questions remain unresolved. First, the timing of the cessation of autumn oviposition and resumption of spring activity is poorly characterised across latitudes. While photoperiod remains the primary diapause cue [12,13], thermal constraints and population-specific adaptations might create substantial local variation. Second, the spatial extent and intensity of egg-laying winter activity along latitudinal gradients have never been systematically quantified with standardised protocols. Data are scattered across agencies using heterogeneous trap types, deployment schedules, and reporting standards.

Third, temporal trends lack rigorous assessment: if climate warming is enabling extended seasons or relaxing diapause, we would expect increasing ovipositing winter activity over time, yet disentangling climate-driven trends from population expansion dynamics and evolving surveillance protocols remains methodologically challenging. Finally, the potential asymmetry between autumn and spring activity, whether pre-diapause oviposition intensity matches post-diapause emergence patterns, remains unquantified, despite implications for understanding overwintering mortality and early-season dynamics.

Here we present the first coordinated assessment of *Ae. albopictus* egg-laying winter activity across spatial and temporal scales in temperate Europe, addressing two complementary objectives: (i) quantify winter ovitrap positivity from October to May across a latitudinal gradient (35-48°N) spanning Italy, France, Switzerland, and Austria during 2024-2025, assessing the relative importance of photoperiod, temperature, and precipitation while testing whether

southern populations exhibit year-round activity; (ii) analyze 15 years (2011-2025) of winter surveillance data from Emilia-Romagna region (northern Italy) to quantify temporal trends and assess whether winter activity is increasing. By uniforming the sampling period and frequency across all sites, we mitigated the methodological heterogeneity that has hindered previous synthesis efforts, providing the first continental-scale evidence for substantial, structured, and potentially increasing winter activity in *Ae. albopictus* populations.

To further contextualise these findings within the broader European distribution of *Ae. albopictus*, we complement our harmonised field surveillance with a descriptive phenological analysis of adult observations from the Mosquito Alert citizen science platform (www.mosquitoalert.com, [17]). Using expert-validated reports spanning 2020–2024 across Europe, we explored the large-scale seasonal phenology of the species along a latitudinal gradient, examining how the timing and duration of the adults' active season vary with latitude and whether cold-season observations are detectable. While citizen science data are subject to spatial and temporal biases in reporting effort and cannot substitute for the controlled protocols underpinning our primary objectives [18], they provide a continental-scale observational backdrop against which the patterns documented in our network can be interpreted. Together, these complementary approaches, controlled ovitrap surveillance and citizen science occurrence data, offer an unusually comprehensive view of *Ae. albopictus* winter activity across temperate Europe.

2. Materials and methods

2.1 Data Collection

2.1.1 Continental-Scale Analysis (Latitudinal Gradient)

We analysed winter ovitrap monitoring data from 14 locations spanning a latitudinal gradient across southern and central Europe (38.1°N to 48.6°N; Fig. 1A), including sites in Italy (n=7), France (n=4), Austria (n=2), and Switzerland (n=1). The monitoring was conducted during the autumn-winter-spring period, from October 2024 (week 44) to May 2025 (week 24), encompassing the period of the year, in temperate Europe, of theoretical absence of the adults due to the population overwintering at the egg stage. The sampling was carried out by a consortium of research groups and public agencies with established expertise in mosquito surveillance (Tab. 1). Each partner oversaw sampling within its respective urban area, implementing an identical field protocol to ensure methodological comparability across countries. Sampling sites within each city were chosen to represent urban environments containing green areas, such as small parks, residential courtyards, or tree-lined streets. These habitats were selected because they constitute common oviposition environments for *Ae. albopictus* and provide microclimatic buffering during winter. A sampling “site” was defined as a single, georeferenced point within the urban areas (WGS 84 reference system; EPSG 4326). At each sampling site, five ovitraps were deployed and spaced approximately fifty meters apart. Partners conducted weekly visits throughout the monitoring period. During each weekly visit, field teams collected the oviposition substrate from every ovitrap and immediately replaced it with a new substrate to ensure uninterrupted monitoring. The ovidepositing substrates were transported to the laboratory on the same day. When eggs were not detected on a ovidepositing substrate, the partner responsible for that site conducted an additional larval survey in the surrounding area. This procedure follows the rationale outlined in previous observations of homodynamic overwintering populations in southern Europe [9]. Due to the implementation of this monitoring effort into progressed entomological surveillance activities and network, it was not possible to standardise the volume of the ovitraps and the ovidepositing substrate across the partners.

7

Table 1. Cities included in the latitudinal transect and corresponding partner institutions.

Country	City	Partner Institution	Number of ovitraps for each location	Ovitrap volume (litres)	Ovideposition substrate
France	Strasbourg	University of Strasbourg	5	3	polystyrene square (5 × 5 × 2 cm)
France	Montpellier	Altopictus	20	3	polystyrene square (5 × 5 × 2 cm)
France	Bordeaux	Altopictus	20	3	polystyrene square (5 × 5 × 2 cm)
France	Bayonne	Altopictus	20	3	polystyrene square (5 × 5 × 2 cm)
Switzerland	Allschwil	Swiss TPH	5	0.4	masonite stick
Austria	Vienna	AGES	5	1	masonite stick
Austria	Graz	AGES	6	1	masonite stick
Italy	Trento	MUSE	5	0.4	masonite stick
Italy	Modena	Centro Agricoltura Ambiente	5	0.4	masonite stick
Italy	Siena	IZS Lazio–Toscana	5	0.4	masonite stick
Italy	Rome	La Sapienza University	5	0.4	masonite stick
Italy	Fondi	IZS Lazio–Toscana	5	0.4	masonite stick
Italy	Bari	University of Bari	5	0.4	masonite stick
Italy	Palermo	IZS Sicilia	5	0.4	masonite stick

8

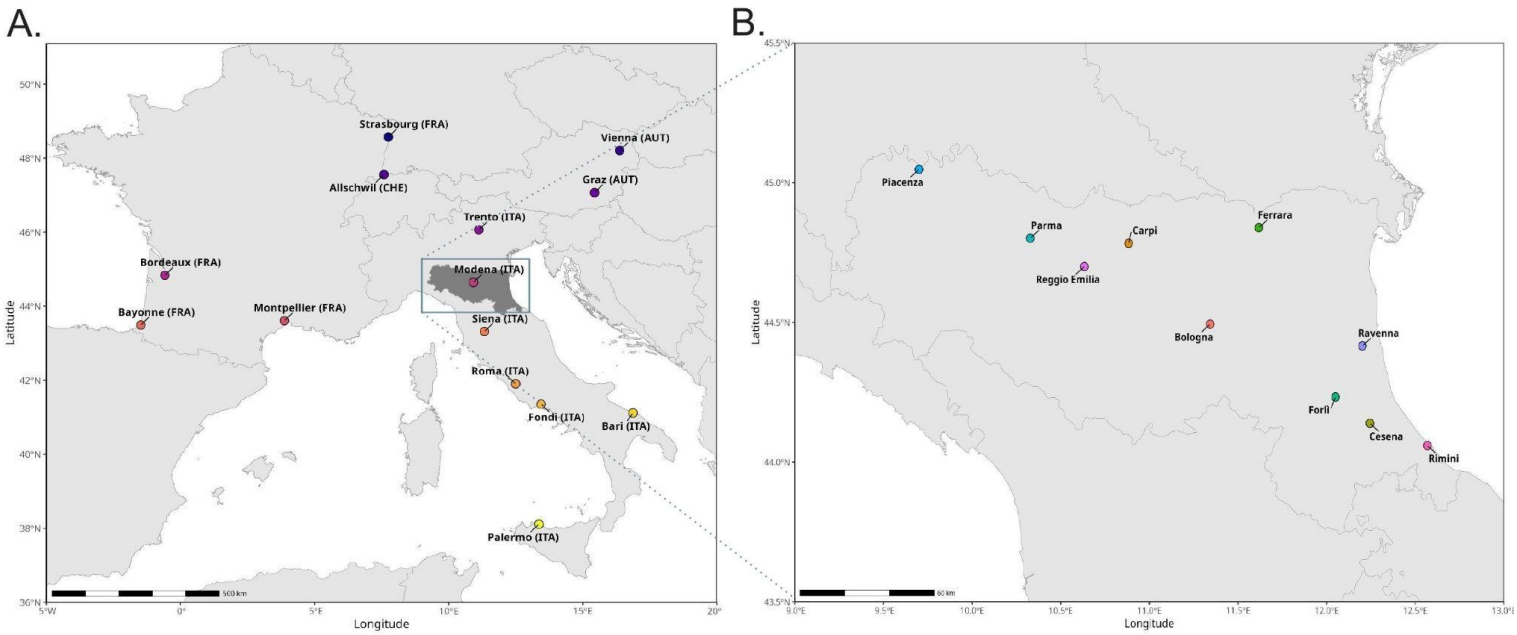

214 **Figure 1. A)** Map of the 14 monitoring sites included in the winter 2024–2025 oviposition study. Locations
215 span a wide latitudinal gradient (approximately 38°–48° N) and include cities in France, Italy, Austria, and
216 Switzerland. The grey region highlights the location of the Emilia-Romagna region in Italy; **B)** Map of the
217 10 municipalities' sites in Emilia-Romagna (Italy) included in the winter 2011–2024 oviposition study.

218 2.1.2 Regional-Scale Analysis (Temporal gradient)

219 We analysed long-term ovitrap monitoring data from 10 municipalities in Emilia-Romagna (110
220 ovitraps), northern Italy (44-45°N), spanning 15 monitoring seasons (2011-2025; Fig. 1B; Tab.
221 2). The ovitrap type employed was a 1.4 L cylindrical black plastic container holding about 900-
222 1000 mL of tap water and a strip of masonite (15 × 2.5 cm) as an egg deposition substrate.
223 Ovitraps were sampled fortnightly during the autumn-winter-spring period (from October to the
224 end of May), using standardised ovitrap management protocols [19] and validating the data after
225 each sampling. Eggs present on the masonite strips were counted through a stereo-microscope
226 by the Regional Agency for Prevention, Environment and Energy of Emilia-Romagna, and
227 subsequently, data were published on the institutional website www.zanzaratigreonline.it.

9

Table 2. Winter surveillance coverage by municipality in Emilia-Romagna, Italy (2011–2025).

Municipality	Longitude	Latitude	Years monitored	Total trap-weeks
Piacenza	9.70	45.0	16	221
Parma	10.3	44.8	13	174
Reggio Emilia	10.6	44.7	16	220
Carpi	10.9	44.8	16	223
Bologna	11.3	44.5	15	200
Ferrara	11.6	44.8	16	222
Forlì	12.0	44.2	16	228
Ravenna	12.2	44.4	16	224
Cesena	12.2	44.1	16	223
Rimini	12.6	44.1	16	218

10

2.2 Predictor Variables

Weekly climate variables were extracted from ERA5-Land reanalysis [20] data at 0.1° spatial resolution for both analyses. We used minimum weekly temperature rather than mean temperature to better capture cold extremes that limit mosquito activity [10], and cumulative weekly precipitation (mm). Climate data were extracted for each monitoring location, with coastal gaps filled using a 5×5 cell focal mean.

For the continental analysis, photoperiod (day length in hours) was calculated for each location and week using the geosphere R package [21], based on latitude and day of year. Based on mosquito development biology and preliminary analyses, we created lagged climate variables to account for delayed effects [22,23]. Temperature and precipitation lags of 1, 2, and 3 weeks were calculated within each location (or municipality) using proper time-lag functions to avoid spurious temporal autocorrelation.

2.3 Statistical Analysis

2.3.1 Collinearity Assessment

Prior to model fitting, we assessed multicollinearity among temperature lags using correlation matrices. Temperature lags exhibited moderate to high correlations ($r = 0.79–0.88$ in the continental dataset; $r = 0.22–0.75$ in the regional dataset). In contrast, precipitation lags showed negligible correlation ($|r| < 0.10$ in both datasets). Based on these diagnostics and biological rationale, we selected lag-3 minimum temperature as the primary temperature predictor for both analyses to minimise collinearity while retaining biological interpretability.

2.3.2 Continental-Scale Model (Latitudinal Gradient)

We modelled ovitrap positivity (presence/absence of eggs) for each location using generalised additive models (GAMs) with a binomial family and a logit link, implemented in the mgcv package (v1.9-3) in R (v4.5.1). The full initial model included a smooth term (thin-plate spline, k=10) for 3-week lagged temperature (tas_lag3), selected a priori based on collinearity diagnostics; linear terms for current precipitation and precipitation lags 1, 2 and 3 weeks; a smooth term for photoperiod (k=10); and random effects for location (12 levels, excluding Vienna and Siena whose ovitraps were never positive) to account for unmeasured spatial heterogeneity, different number of deployed traps (France: 20 traps; other countries: 5 traps; Tab. 1), and different number of ovidepositing substrate.

Model selection was carried out using Akaike Information Criterion (AIC), likelihood ratio tests (LRT), examination of concurvity (generalised collinearity for GAMs), and basis dimension adequacy (k-index tests; k increased until $p > 0.01$ or k-index > 1.0).

2.3.3 Regional-Scale Model (temporal gradient)

For the Emilia-Romagna dataset, we modelled the number of positive ovitraps out of total ovitraps deployed in a municipality using GAMs with binomial response (or quasibinomial if overdispersed, φ > 1.5) and logit link. Given the narrow latitudinal range (~1°), photoperiod was not included as a predictor; within-season timing was instead captured by a cyclic cubic regression spline on a “winter week” index (week 1–31, from mid-October to late May), using boundary knots at weeks 1 and 31 to ensure continuity across season transitions. A binary season indicator (“period”: Autumn vs. Spring) was included to account for the marked difference in baseline activity between the October–December and January–May sub-periods (before and after the winter solstice in the Northern hemisphere). The 3-week lagged minimum temperature was included in the full model alongside year and seasonal predictors. Because s(year) as a smooth spline can absorb inter-annual temperature signals, temperature was evaluated in the context of the full model before any removal. Precipitation lags were retained if statistically significant. Model selection followed the steps described in section 2.3.2.

To evaluate temporal trends in winter oviposition activity, we computed observed mean ovitrap positivity per winter season across all municipalities, both for the full monitoring period and separately for the autumn (October–December) and spring (January–May) sub-periods. Linear regression models were fitted to these annual means as a function of calendar year, and statistical significance was assessed via t-tests. The interaction between year and season (autumn vs. spring) was tested in a combined model including both sub-periods to assess whether temporal trends differed between them.

2.3.4 Models Diagnostics and Validation

For both continental and regional scale analyses, the performance of the models was evaluated using adjusted R^2 and deviance explained. For the continental model only, location-specific performance metrics (the area under the ROC curve - AUC, sensitivity, specificity, precision, F1 score) were also computed to assess spatial variation in model accuracy.

2.3.5 Trapping effort optimisation

To inform surveillance planning in similar temperate regions, we estimated minimum trap requirements for reliable winter detection based on empirical positivity rates from the 14-year Emilia-Romagna dataset. For each period, we calculated the number of traps required to achieve specified detection probabilities (50%, 80%, 95%, 99%) using the binomial sampling framework: for a given positivity rate p and target detection probability D (defined as probability of recording at least one positive trap), the required number of traps n is derived from $1 - (1 - p)^n = D$, solving for $n = \log(1 - D) / \log(1 - p)$. We then assessed the adequacy of our actual deployment (median 10 traps per municipality-week) by calculating the proportion of location-year observations that achieved ≥80% and ≥95% detection probability given observed positivity rates.

12

2.4 Citizens Science observations

Occurrence data for *Ae. albopictus* were obtained from the Mosquito Alert citizen science platform covering Europe over the period 2020–2025. Data retrieval was performed via a custom R script utilising the *download.ma_verified_records* function (freely available at https://github.com/EleonoraLongo/mosquitoalert_italy). Specifically, the script was configured to extract georeferenced photographic records of adult mosquitoes across 46 European countries (encompassing European Union member states, the United Kingdom, European Free Trade Association countries, the Balkans, and microstates). To specifically investigate cold-season and transitional dynamics, the query was restricted to the months of October through June. Following data retrieval, post-processing steps were applied to clean and structure the data, allowing it to be exported as a standard CSV file for downstream analysis. Only georeferenced photographic observations validated by expert entomologists were retained, and records for 2025 were excluded due to the limited sample size. To visualise seasonal phenology across the latitudinal range of the species, records were aggregated into 1° latitude bins and calendar months. To account for the marked interannual growth in reporting effort, relative frequency was computed via a two-step normalisation: monthly counts were first expressed as a proportion of annual totals within each year × latitude bin, then averaged across years so that each year contributed equally to the seasonal signal regardless of absolute reporting volume. The resulting metric reflects the mean proportion of reports attributable to each month within a latitude band, independently of sampling and dissemination efforts. Seasonal phenology was visualised as a bubble plot with month on the x-axis (ordered October–September to centre the winter period) and latitude on the y-axis, where bubble size encodes relative frequency, and transparency encodes mean annual observations per cell as an indicator of estimate reliability. A winter subset (December–March) was additionally disaggregated by country to explore spatial heterogeneity in cold-season reporting.

All analyses were conducted in R v4.5.1 [17]. The data and the R scripts used for all the analyses are available in the GitHub repository https://github.com/danddr/albo_winter_monitoring.git.

3. Results

Across the 14 continental monitoring sites, a total of 345 trap-weeks of data were collected between October 2024 and May 2025, following the exclusion of Siena (Italy) and Vienna (Austria), where no positive ovitraps were recorded throughout the monitoring period. Overall, ovitrap positivity across the remaining 12 locations varied markedly, with sites in France and southern Italy showing positive ovitraps during the autumn, with the exception of Palermo (Italy) in which the presence of eggs was detected also in January 2025. The northern sites (Allschwil, Strasbourg, Graz) showed a complete absence of eggs during the winter months. Positivity was highest during October–November and April–May at most locations, and declined to its seasonal minimum in December–February, particularly above 44°N.

In the Emilia-Romagna regional dataset, 1,999 trap-weeks were available across 10 municipalities and 14 winter seasons (2011/12 to 2024/25). Overall, ovitrap positivity across the

13

full dataset was 50.2%, with substantial inter-annual variation: mean seasonal positivity ranged from 12.1% (2011/12) to 27.2% (2022/23), with an overall mean of 20.9% across all seasons and municipalities. Within-season patterns were consistent across years, with autumn (October–December) recording substantially higher positivity than spring (January–May) in all 14 seasons.

3.1 Continental scale analysis (Latitudinal Gradient)

Stepwise model selection began with a full model including minimum temperature lag-3 (as a smooth), precipitation terms (current week and lags 1–3), photoperiod (as a smooth), and location random effects (AIC = 152.02, R^2 = 0.680, deviance explained = 67.9%). All four precipitation terms were non-significant and were sequentially removed without significant loss of fit (LRT p = *ns* for removal of all four; AIC improved to 149.16). The smooth term for 3-week lagged temperature had effective degrees of freedom (EDF) = 1.0, indicating a linear relationship; simplification to a parametric term yielded no change in fit (ΔAIC < 0.01, LRT p = 0.013). The final model structure was:

$$\text{logit}(P(\text{ovitrap positive})) = \beta_0 + \beta_1(\text{tas\_lag3}) + f(\text{photoperiod}) + u(\text{location}) \quad \textbf{Eq. 1}$$

where tas_lag3 = minimum temperature 3 weeks prior (linear), f(photoperiod) = smooth function of day length, and u(location) = random intercept for location.

The final model (Eq.1) explained 66.3% of deviance (adjusted R^2 = 0.664, AIC = 149.16, n = 345). All retained predictors were statistically significant (Tab. 3). Model diagnostics indicated adequate basis dimensions and acceptable concurvity (worst case = 0.523 for photoperiod). Overdispersion was negligible (φ = 0.378), confirming that the binomial family was appropriate.

Table 3. Summary of the final generalised additive model (GAM) for continental-scale ovitrap positivity. Family: binomial; link: logit; n = 345 trap-weeks across 12 locations. Parametric terms: coefficient estimate, standard error (SE), z-statistic and p-value. Smooth terms: effective degrees of freedom (EDF), reference degrees of freedom (Ref. df), χ^2 statistic and p-value. Significance codes: *** p < 0.001. Dashes (—) indicate statistics not applicable to model fit indices.

Term	Estimate/ EDF	SE / Ref. df	z / χ^2	p-value
A. Parametric coefficients				
(Intercept)	-6.495	1.113	-5.84	5.27×10^{-9} ***
min. temperature, 3-week lag; °C)	0.515	0.107	4.74	2.15×10^{-6} ***
B. Smooth terms				
s(photoperiod, k = 10)	3.144	3.902	38.10	$< 2 \times 10^{-16}$ ***
s(location, bs = "re")	8.956	11	26.12	8.13×10^{-4} ***

15

The temperature lag-3 effect exhibited near-zero predicted probability at minimum temperatures below 0°C and approached higher probability above 15°C when other predictors were held at median values (Fig. 2A). Each 1°C increase in minimum temperature increased the odds of detection by approximately 63%

Photoperiod exhibited a non-linear effect (Fig. 2B), characterised by high probability at extreme short (<9 hours) and long (>14 hours) day lengths, with lower probabilities during intermediate autumn (11-13 hours) photoperiods.

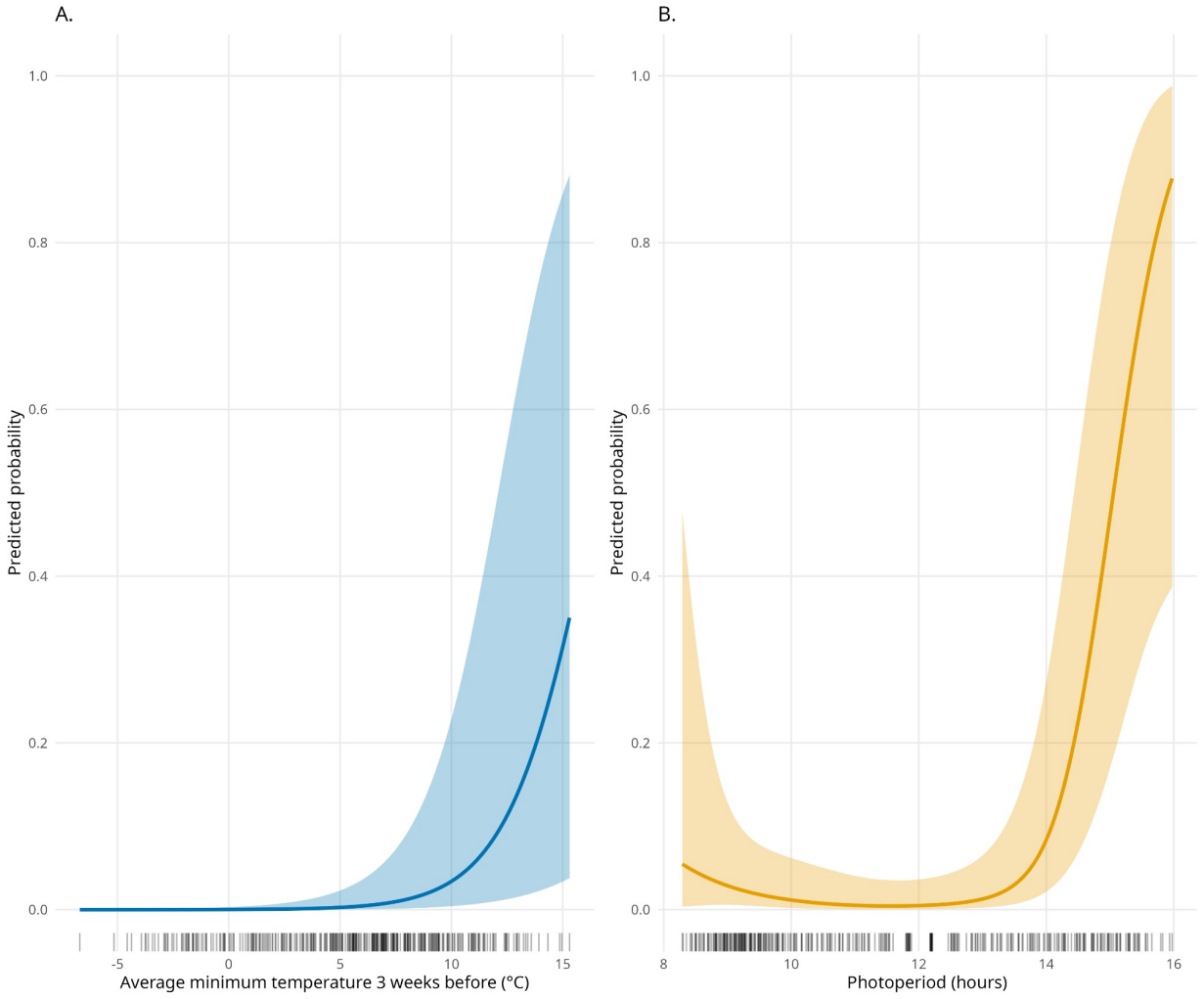

Figure 2. Partial dependence plots from continental-scale analysis showing marginal effects of (A) 3-week lagged minimum temperature and (B) photoperiod on predicted probability of ovitrap positivity. All other predictors held at median values; location random effects excluded. Shaded regions = 95% confidence intervals. Rug plots show data distribution. Model: GAM with $R^2 = 0.664$, n = 345 trap-weeks.

16

Two-dimensional predictions in photoperiod × temperature space revealed strong synergistic effects (Fig. 3). Marginal predictions (location random effects excluded) showed three distinct zones: High probability zone (P > 0.8): photoperiod 13–16 hours and minimum temperature lag-3 > 10°C, representing optimal autumn and spring conditions (top-right); Moderate probability zone (P> 0.5): photoperiod 8–10 hours and minimum temperature lag-3 > 10°C (bottom right), representing coastal and southern location autumnal conditions; Low probability zone (P < 0.2): photoperiod < 14 hours or minimum temperature lag-3 < 10°C, representing diapause-inducing or thermally limiting conditions.

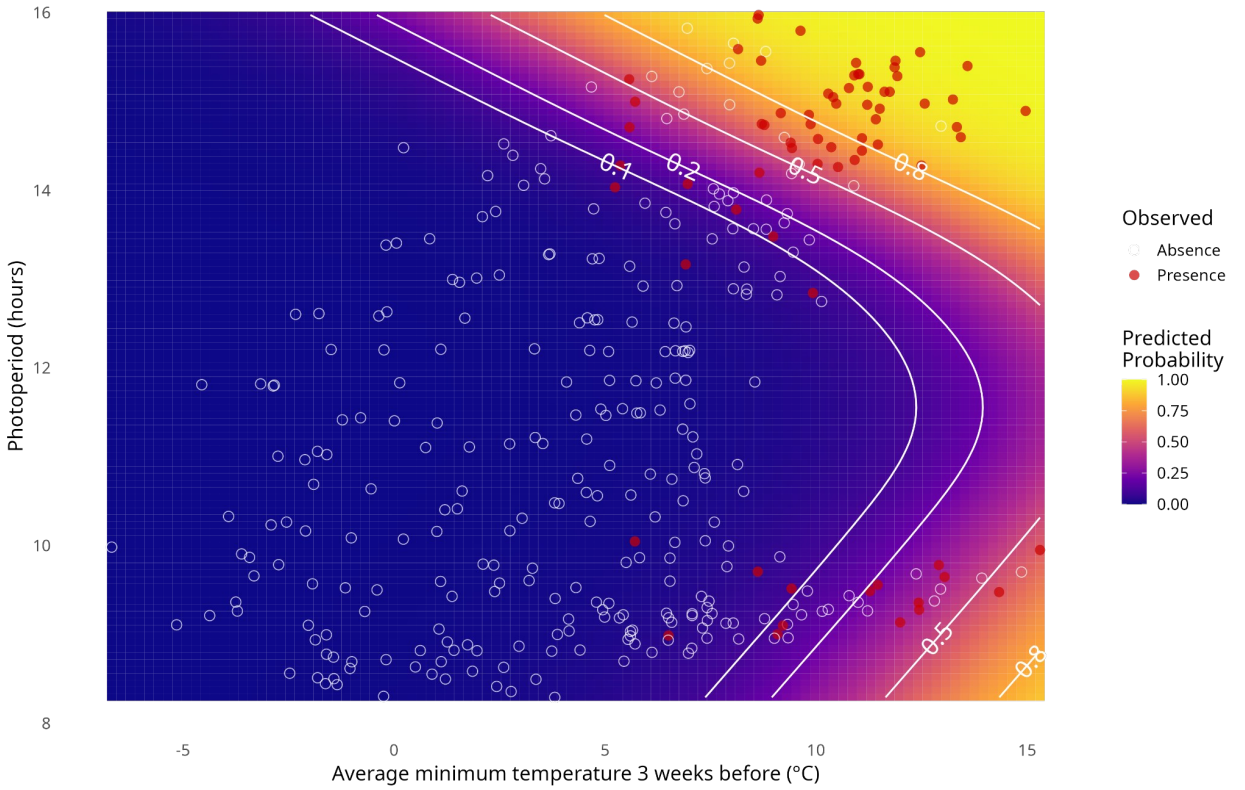

Figure 3. Two-dimensional predictions in photoperiod × temperature space (continental analysis). Marginal effect heatmap with location random effects excluded. White contour lines = 10%, 20%, 50%, 80% probability thresholds. Points = observed presences (filled red) and absences (open white). City-specific two-dimensional predictions in photoperiod × temperature space are available in Fig. SM1.

Location random effects were substantial (EDF = 8.871, representing unique intercepts for most locations), indicating that even after accounting for temperature lag-3 and photoperiod, significant unmeasured spatial variation persists. Location-specific predictions revealed strong north–south gradients in baseline probability, with southern locations (Palermo, Bari) maintaining higher probabilities across a broader range of conditions, e.g., even with minimum temperature lag-3 < 10°C, than northern locations (Allschwil, Strasbourg, Graz; Fig. 4).

17

Overall model performance was strong: ROC AUC = 0.972, accuracy = 92.5%, sensitivity = 96.4%, specificity = 77.5%, precision = 94.3%, and F1 score = 0.953. Per-location performance varied across sites, consistent with differences in sample size, seasonal prevalence, and local climate variability (Tab. SM2-3).

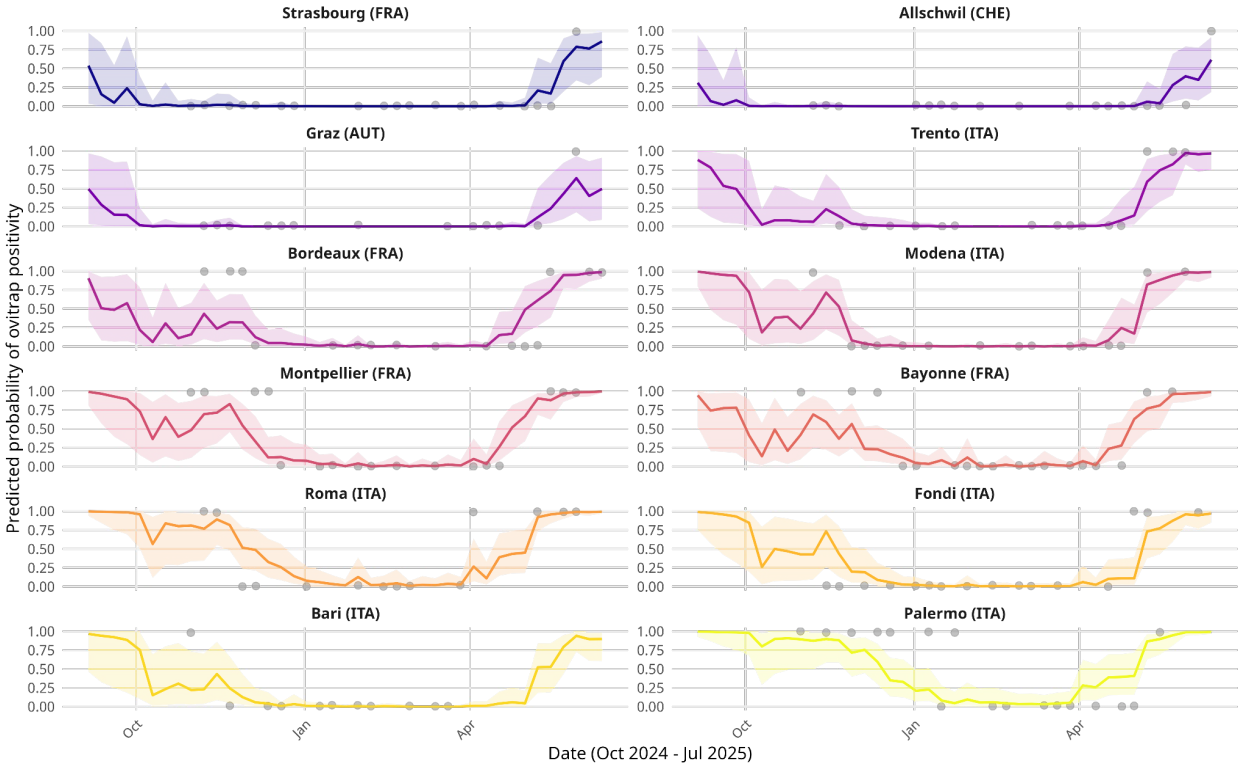

Figure 4. Seasonal predictions for 2024-2025 monitoring period (continental analysis). Lines = predicted probability with 95% confidence bands. Points = observed presences (1) and absences (0) with vertical jitter. Colours = locations ordered by latitude (north to south). Model captures bimodal seasonal pattern and latitudinal variation in winter activity.

18

3.2 Regional-Scale Analysis (Temporal gradient)

In the full Emilia-Romagna model, the smooth of minimum temperature lag-3 was not statistically significant (EDF = 3.93, F = 1.83, p = 0.104), despite a marginally significant LRT when the term was removed (ΔDeviance = 23.1, F = 2.21, p = 0.040). Given the non-significance of the smooth in the full model summary and its high concurvity with *winter_week* (worst-case = 0.85), temperature was excluded from the final model. As a consequence, the final regional model (Emilia-Romagna, 2011–2025, n = 1,999 trap-weeks) was

$$\text{logit}(n_{pos} / n_{ovi}) = f(\text{winter\_week}) + \beta_1(tp) + \beta_2(tp\_lag1) + \beta_3(tp\_lag2) +$$

$$\beta_4(tp\_lag3) + \beta_5(\text{period}) + f(\text{year}) + u(\text{municipality}) \quad \textbf{Eq. 2}$$

where n_{pos} and n_{ovi} are the number of positive ovitraps and the total number of ovitraps deployed, respectively; f(winter_week) = cyclic cubic spline (k=24) for seasonal pattern; tp, tp_lag1, tp_lag2, tp_lag3 = cumulative precipitation at lags 0–3 weeks (linear); period = binary Autumn/Spring indicator; f(year) = thin-plate spline (k=10) capturing inter-annual variation; and u(municipality) = municipality random intercepts (n=10). The final model explained 75.2% of deviance (adjusted R^2 = 0.830) and was fit using a quasibinomial family to account for moderate overdispersion (φ = 1.775).

The seasonal smooth (cyclic cubic spline, k=24) captured complex within-season variation (EDF = 13.398, F = 140.1, $p < 2\times10^{-16}$), with higher activity during autumn (October–November) and reduced activity during winter (December–February; Fig. 5A). All four precipitation terms showed consistent negative associations with ovitrap positivity, with effect sizes increasing from current week to lag-2 (Tab. 4). Each 10 mm of cumulative weekly rainfall reduced the odds of ovitrap positivity by approximately 5–7%, depending on the lag (Fig. 5B).

The binary period indicator confirmed a markedly lower baseline in spring relative to autumn, consistent with the seasonal decline in egg-laying activity following population peaks in summer (Fig. 5C). The k-index diagnostic for the seasonal smooth was borderline (k-index = 0.95, p = 0.08), indicating near-adequate basis dimension; however, increasing k beyond 10 was not feasible given the 14-year time series and the risk of overfitting.

Table 4. Summary of the final generalised additive model (GAM) for Emilia-Romagna regional ovitrap positivity. Family: quasibinomial; link: logit; n = 1,999 trap-weeks across 10 municipalities and 14 winter seasons (2011/12–2024/25). Response: number of positive ovitraps out of total ovitraps deployed per municipality-week. Parametric terms: coefficient estimate, standard error (SE), t-statistic and p-value. Smooth terms: effective degrees of freedom (EDF), reference degrees of freedom (Ref. df), F-statistic and p-value. Significance codes: *** p < 0.001, ** p < 0.01. Dashes (—) indicate statistics not applicable to model fit indices.

Term	Estimate / EDF	SE / Ref. df	t / F	p-value
A. Parametric coefficients				
(Intercept)	-0.793	0.178	-4.45	9.19×10^{-6} ***
tp (precip., lag 0; mm)	-0.00502	0.00173	-2.9	0.0038 **
tp_lag1 (precip., lag 1; mm)	-0.00648	0.00178	-3.64	2.78×10^{-4} ***
tp_lag2 (precip., lag 2; mm)	-0.00817	0.00188	-4.35	1.44×10^{-5} ***
tp_lag3 (precip., lag 3; mm)	-0.00731	0.00199	-3.67	2.46×10^{-4} ***
periodSpring (ref.: Autumn)	-1.227	0.192	-6.4	1.92×10^{-10} ***
B. Smooth terms				
s(winter_week, cc, k = 24)	13.398	22	140.1	$< 2 \times 10^{-16}$ ***
s(year, k = 10)	8.083	8.736	27.15	$< 2 \times 10^{-16}$ ***
s(location, bs = "re")	8.1	9	8.01	$< 2 \times 10^{-16}$ ***

20

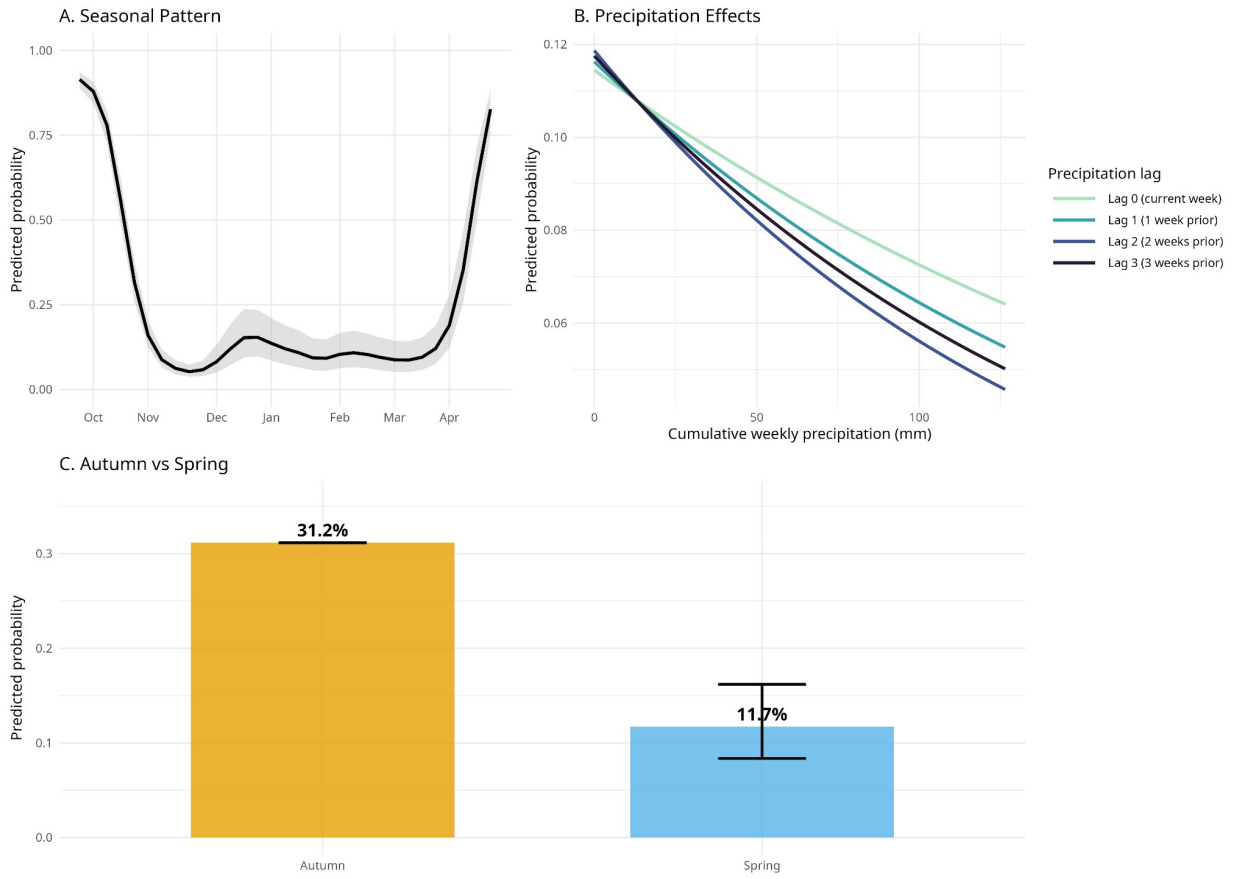

Figure 5. Partial dependence plots of the temporal gradient analysis of winter ovitrap positivity, Emilia-Romagna (2011–2025). (A) Smooth inter-annual effects (year) with 95% confidence intervals (EDF = 8.08). (B) precipitation lagged effects, C) seasonal differences before and after the winter solstice.

Inter-annual variability was substantial and non-monotonic. The inter-annual smooth (s(year), EDF = 8.083) captured substantial year-to-year variation in ovitrap positivity beyond seasonal and climatic patterns. A linear regression on the observed annual mean positivity showed a positive but non-significant trend (slope = 0.008 per year, SE = 0.0027, t = 1.89, p = 0.083, R^2 = 0.23). When analysed separately by seasonal period (Fig. 6), the Spring sub-period showed a statistically significant increasing trend (slope = 0.0068 per year, SE = 0.0022, t = 3.04, p = 0.010, R^2 = 0.44), while the Autumn sub-period did not (slope = 0.0132 per year, SE = 0.0073, t = 1.80, p = 0.098, R^2 = 0.21). The interaction between year and period was not significant (p = 0.577), indicating parallel but non-overlapping trends in the two sub-periods.

3.4 Trapping effort optimisation

Based on observed positivity rates across 270 location-year combinations (2011–2024), minimum trap requirements for reliable detection (80% probability) differed substantially between periods: 4 traps for autumn (mean positivity 37.6%, SD=13.6%) versus 13 traps for spring (mean positivity 12.2%, SD=6.4%). For high-confidence detection (95%),

21

requirements increased to 7 traps (autumn) and 24 traps (spring). The actual deployment (median 10 traps per municipality-week, interquartile range 10–10) substantially exceeded autumn requirements, with 91.9% of observations achieving ≥80% detection probability. In contrast, spring surveillance was underpowered: only 32.6% of observations met the 80% detection threshold (Fig. SM4).

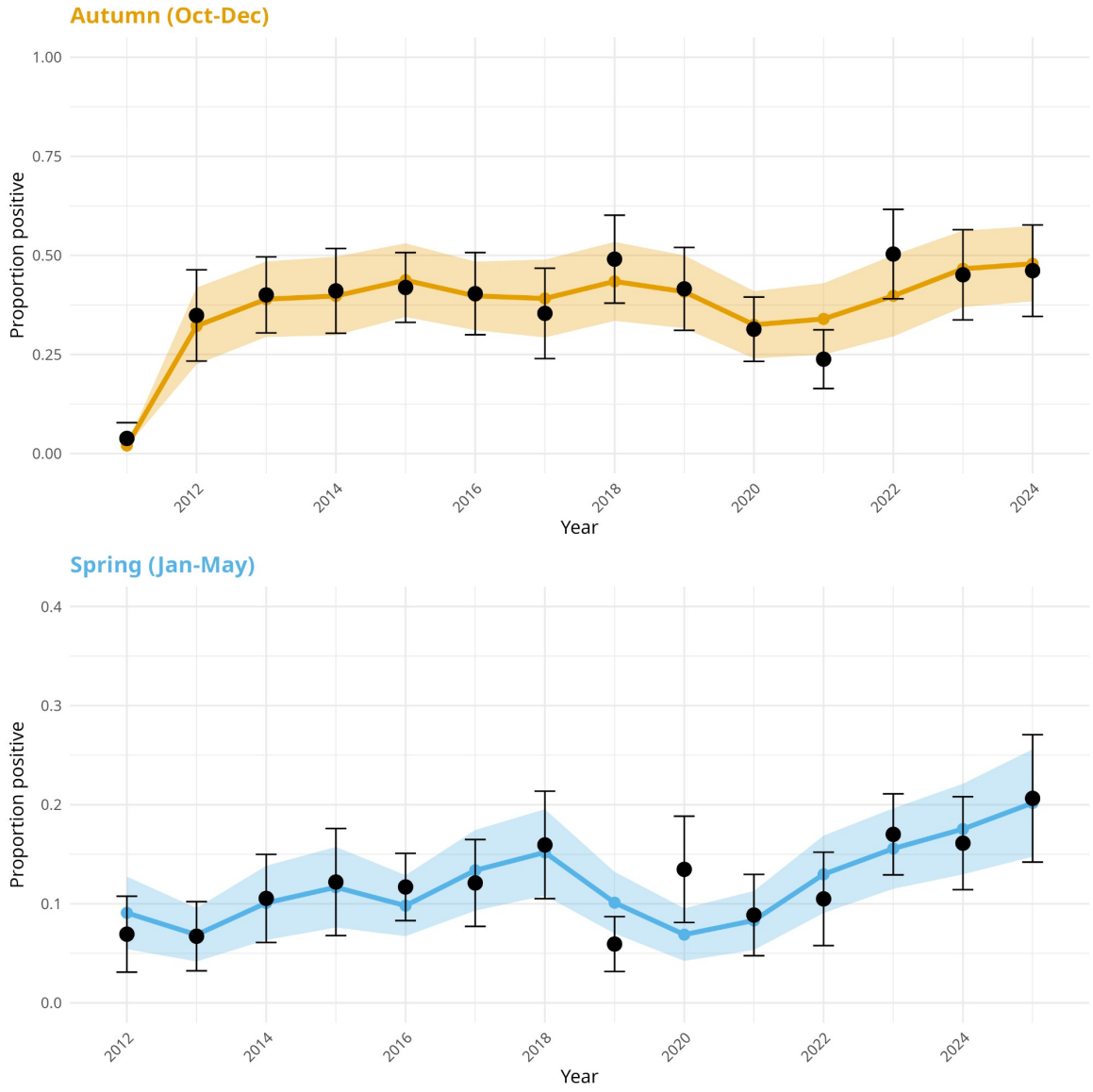

Figure 6. Temporal trends in winter ovitrap positivity, Emilia-Romagna (2011–2025). (A) Smooth inter-annual effect s(year) with 95% confidence intervals (EDF = 8.08). (B) Observed vs. predicted annual means ± 95% CI by season (Autumn: October–December; Spring: January–May). Dashed lines show fitted linear trends: Spring slope = 0.007/year (p = 0.010); Autumn slope = 0.013/year (p = 0.098). Model R^2 = 0.830, n = 1,999 trap-weeks.

22

3.4 Citizens Science observations

A total of 6,512 expert-validated *Ae. albopictus* records spanning 34°N–52°N were analysed across 2020–2024, with reporting density concentrated between 40°N and 44°N, broadly corresponding to the Iberian Peninsula and northern Italy (Fig. 7A). The seasonal phenology plot revealed a clear unimodal activity pattern at core latitudes, with relative frequency peaking between July and October and declining sharply through winter. Notably, the highest relative frequency of cold-season reports (December–March) originated from northern latitude bins (48–52°N) rather than from the warmer southern range, a pattern that was not evenly distributed across countries and was characterised by low mean annual counts (Fig. 7B).

Figure 7. Descriptive phenology of *Aedes albopictus* across Europe based on Mosquito Alert citizen

science data (2020–2024). (A) Bubble plot of mean relative frequency of validated occurrence reports by calendar month (x-axis, ordered October–September) and 1° latitude bin (y-axis). Bubble size represents relative frequency, i.e. the mean proportion of annual reports attributable to each month within a latitude band, effort-corrected by averaging across years. Bubble transparency reflects mean annual observations per cell, serving as an indicator of estimate reliability (more transparent = fewer observations). (B) Winter subset (December–March) disaggregated by country, with month encoded by colour, illustrating spatial heterogeneity in cold-season reporting patterns.

23

4. Discussion

4.1 Continental scale

Despite the well-documented presence of diapausing *Ae. albopictus* populations in temperate Europe, winter egg-laying activity patterns remain almost completely unstudied [11,15,16]. Existing surveillance programs operate primarily from May to October, reflecting the historical assumption that winter activity is negligible and that diapause represents complete dormancy. Building on previous efforts [11], this study represents the first coordinated assessment of winter *Ae. albopictus* activity at both continental and regional scales, demonstrating that winter monitoring is essential for understanding population persistence, invasion dynamics and potential disease transmission risk in temperate regions.

Our continental-scale dataset (2024-2025, n = 345 trap-weeks across 12 locations) represents the first systematic winter monitoring effort spanning a 13° latitudinal gradient. The most striking finding was the substantial autumn activity in France and southern locations of the study area, which maintained detectable activity throughout the winter months, when northern sites showed near-complete cessation.

The dominant role of photoperiod (explaining 23% of deviance) aligns closely with diapause biology: day length cues regulate diapause entry and exit, creating predictable autumn and spring activity windows across the latitudinal gradient [13]. The non-linear photoperiod effect (EDF = 3.154) is particularly informative when interpreted in conjunction with the two-dimensional heatmap (Fig. 3). The high-probability zone ($P > 0.8$) corresponds to photoperiods of 13–16 hours combined with 3-week lagged minimum temperatures above 10°C, capturing the autumn and early-spring window when day length is sufficiently long to avoid or terminate diapause and thermal conditions remain permissive. Crucially, a moderate-probability zone ($P > 0.5$) also emerges at short photoperiods (8–10 hours), when minimum temperatures exceed 10°C (bottom-right corner of Fig. 3), reflecting positive trap detections in mid-to-late autumn when temperatures are still relatively high despite shortening days. This non-linearity may reflect the high adult densities reached during summer and early autumn, which can sustain detectable oviposition in ovitraps into mid- and late autumn, producing a more complex response surface than a simple diapause threshold model would predict. In contrast, spring recovery is likely slower, as post-diapause populations need time to produce enough adult females for oviposition to become detectable in ovitraps. Activity falls to low probability ($P < 0.2$) when 3-week lagged minimum temperatures drop below 10°C, regardless of photoperiod, or when day lengths fall outside the 8–16 hour window under thermally limiting conditions.

Temperature effects, while statistically significant, were thus secondary to photoperiod, modulating activity within photoperiod-constrained windows rather than driving the overall seasonal pattern. Indeed, low temperatures typically delay development and thereby increase the number of short days spent during the photosensitive stage, thereby increasing the diapause incidence [13]. These temperature associations should nonetheless be interpreted cautiously, given our single-season data; interannual validation is needed to confirm whether the 10°C minimum temperature threshold represents a consistent biological limit or reflects the particular thermal conditions of the 2024–2025 monitoring season.

24

Substantial spatial heterogeneity persisted even after accounting for photoperiod, temperature, and precipitation (location random effects EDF = 8.61), indicating that local factors such as microclimate, urban heat island effects, habitat availability, or historical colonisation dynamics can substantially modify winter activity potential [24,25]. This spatial complexity is evident in continent-wide citizen science data (Mosquito Alert 2020–2024, n = 6512 validated records): unexpectedly, the highest relative frequency of winter reports (December–March) originated from northern latitudes (48-52°N) rather than warmer southern sites (Fig. 7). However, these northern detections were sparse (low annual counts) and geographically clustered (Fig. 7B), likely reflecting localised persistence in heated indoor urban microrefugia or reporting heterogeneity rather than broad-scale cold adaptation. This disconnect between climatic suitability and observed winter activity underscores the challenge of extrapolating winter ovistrap positivity from continental-scale climate variables alone and highlights the value of location-specific surveillance.

Our findings are in line with previous evidence from central Italy showing that winter oviposition may persist under Mediterranean conditions when photoperiod and minimum temperatures remain permissive [11]. At those latitudes (41-42° N), where day length does not fall below approximately 8 hours of daylight, oviposition has been recorded only under thermally favourable conditions, with daily minimum temperatures remaining above 0°C throughout the winter and a mean minimum temperature of 4.85°C over the three weeks preceding each positive sampling. At the continental scale, our results indicate that winter vector activity in southern Europe and across Mediterranean basin countries is not negligible, particularly during the early and late phases of the winter season, supporting previous reports of homodynamic populations in Spain [15,26] and winter oviposition in Lebanon [27].

4.2 Regional scale

Our 15-year Emilia-Romagna dataset (2011-2025, n = 1,999 trap-weeks) provides the temporal depth unavailable at the continental scale. The dominant signal in the regional model is the strong seasonal pattern captured by the cyclic spline (EDF = 13.4), with autumn (October-December) positivity substantially higher than spring (January–May). We interpret this asymmetry as follows: the late-summer population build-up in *Ae. albopictus* sustains a pool of adults and freshly laid eggs entering the autumn monitoring window, so that, when minimum temperatures remain permissive, as shown in the continental and citizen science analyses, oviposition activity remains relatively high in October-November before declining as winter cold intensifies. Conversely, spring positivity reflects the gradual resumption of activity from a population that has passed through the winter bottleneck, and is thus lower on average.
All four precipitation lags (current week through lag-3) were statistically significant and showed consistent negative effects. We retained all four terms because their low mutual correlations ($|r| < 0.10$) satisfy independence assumptions and the model selection criteria supported their inclusion. We acknowledge, however, that four lags with similarly-signed coefficients of comparable magnitude may partly capture the same multi-week wet episodes rather than strictly independent mechanisms, and future work could explore whether a single aggregate precipitation index performs equivalently.

Inter-annual variation was large and non-linear (EDF = 8.08), and this is arguably the most informative temporal result of the regional analysis. The non-linearity indicates that positivity fluctuates considerably from year to year without following a simple monotonic trajectory, which could explain why the overall annual trend across the full winter season was not statistically significant. Notably, the 2021 anomaly (observed positivity below autumn model prediction) may reflect COVID-19 pandemic disruptions or environmental changes associated with reduced urban activity, though we lack the ovitrap monitoring metadata to test these hypotheses directly.

When the two sub-periods are examined separately, a clearer picture emerges: the spring trend is statistically significant (slope = 0.07/year, $p = 0.010$, $R^2 = 0.44$), whereas the autumn trend is not (slope = 0.004/year, $p = 0.54$, $R^2 = 0.04$). We interpret this divergence as reflecting different processes operating in the two sub-periods. Autumn positivity is largely governed by the carryover of the summer population, which fluctuates year-to-year with late-summer and early-autumn temperatures and other conditions affecting the preceding breeding season; the resulting high inter-annual variance suppresses the power to detect a trend.

Spring positivity, by contrast, integrates the size and physiological state of the overwintering cohort, and its increasing trend could be related to progressively milder late-winter and early-spring conditions that facilitate earlier diapause termination [28], although several caveats apply that compound uncertainty in the spring estimate specifically. First, temperature effects were not significant and showed high concurvity with temporal trends, indicating confounding between climate and year-to-year population variation. Second, while sampling protocols in the region were standardised across the study period, we cannot entirely rule out gradual improvements in trap maintenance, deployment timing, or detection probability as operators gained experience, all artefacts that could contribute to apparent spring increases. Third, and critically, our trap deployment (median 10 per municipality-week) substantially exceeded autumn detection requirements (4 traps for 80% detection probability, with 92% of observations adequately powered), but fell short of spring thresholds (13 traps required, with only 33% of observations achieving 80% detection probability). This differential statistical power provides high confidence in the autumn null result, but introduces sampling uncertainty into the spring trend estimate. The constant autumn-spring asymmetry across all years (period × year interaction $p = 0.58$) and the proportional impact of the 2021 anomaly on both periods argue against major systematic surveillance biases, but the modest spring increase nonetheless warrants cautious interpretation pending replication with adequate trap effort (13-15 per site), detailed trap-level metadata, and independent datasets.

Finally, we emphasise that what we are observing almost certainly reflects the population dynamics of a long-established species rather than ongoing invasion. In Emilia-Romagna, *Ae. albopictus* was first recorded in Bologna city in 1994 [29], nearly two decades before our monitoring period began. By 2011, the species was firmly established across the region. The inter-annual fluctuations documented here are therefore best understood as demographic oscillations of a resident population responding to year-to-year climatic variability, rather than as signals of range expansion or early establishment dynamics. This distinction matters for how vector dynamics in colonised regions are positioned within broader climate attribution frameworks: within an already-established range, the relevant climate signal operates through modulating the magnitude and phenology of resident population fluctuations rather than enabling new colonisation [30–32]. In a region where *Ae. albopictus* has been resident for three decades, it is the inter-annual climatic variability, projected to intensify under future emissions scenarios, that operates as the proximate regulator of population dynamics, and it is therefore

this variability that should anchor surveillance design and public health preparedness in already-colonised areas [33].

4.3 Overall and future perspectives

Taken together, the contrasting results between continental and regional analyses reflect different ecological processes operating at different spatio-temporal scales rather than methodological inconsistencies. At the continental scale, photoperiod-driven diapause regulation dominates across the latitudinal gradient, with temperature modulating activity within photoperiod-constrained windows, suggesting where and when winter activity occurs across Europe. At the regional scale, within a climatically homogeneous area, seasonal weather variability and multi-year population dynamics become more important, though temperature effects remain entangled with temporal trends and seasonal timing. Together, these analyses provide convergent evidence that winter activity is substantial and ecologically structured across temperate Europe, that photoperiod governs seasonal timing at large spatial scales, that local weather, temperature and precipitation modulate activity at finer scales, and that southern populations sustain near year-round activity.

Both analyses carry important limitations that reflect field-wide data gaps rather than methodological flaws. The continental dataset spans a single season, precluding assessment of whether 2024-2025 represents typical or anomalous winter conditions and making interannual validation of photoperiod and temperature thresholds impossible. The regional dataset cannot disentangle the confounded drivers of inter-annual variation, particularly the collinearity between temperature, seasonal timing, and year effects. Additionally, our trap deployment in the Emilia-Romagna region substantially exceeded autumn detection requirements but fell short of spring thresholds, with only 33% of spring observations achieving adequate statistical power. This differential adequacy explains robust autumn results but necessitates cautious interpretation of the modest spring increase, which may reflect sampling uncertainty. These gaps point to clear research priorities: first, replicating the continental survey across a minimum of three to five consecutive winters to distinguish stable spatial patterns from year-specific anomalies. Our empirically-derived trap requirements can provide practical guidance for winter surveillance planning: to achieve an 80% detection probability, 4-7 traps per municipality might suffice for autumn monitoring (October-December) in temperate regions, while spring monitoring (January-May) requires 13-24 traps to compensate for substantially lower activity. Second, conducting controlled mesocosm experiments manipulating photoperiod and temperature in field-derived populations to establish causal thresholds and investing in comparative genetic and physiological studies across populations showing divergent winter activity patterns to assess the contribution of local adaptation, if any.

The public health implications are direct and pressing. Southern European sites maintain substantial winter activity that current May-October surveillance programmes entirely miss, potentially underestimating population persistence and the timing of spring population rebound. While some regions are beginning to extend surveillance (e.g., April-November in Nouvelle-Aquitaine, May-November in Occitanie, France; personal communication AM), these extensions remain fragmented and lack coordination. Our results suggest differentiated surveillance strategies may be appropriate: at northern latitudes (>48°N, exemplified by Austria and Switzerland), standard May-October still monitoring appears sufficient given minimal winter activity; at intermediate latitudes (40-47°N, temperate regions including Emilia-Romagna, Italy), April-December monitoring captures peak late-season activity critical for overwintering

population assessment, while January-April monitoring remains marginal due to low detection probability; at southern latitudes (<40°N, Mediterranean climates), year-round or extended-season surveillance (March-November) is likely necessary to capture persistent winter populations.

However, implementing continent-wide winter surveillance faces practical challenges. Methodological standardisation remains elusive: ovitrap volumes vary from 400mL to 3L, oviposition substrates range from Masonite strips, polystirol floating surfaces, to tongue depressors, and deployment intervals span 1-4 weeks, all of which affect detection sensitivity and comparability. We advocate for a coordinated European surveillance network with standardised protocols (trap specifications, bi-weekly sampling intervals, common data reporting) stratified by latitude and climate to establish baseline winter activity patterns and enable detection of phenological shifts. Finally, if the tentative increasing spring trend observed in Emilia-Romagna reflects a genuine phenological shift, regardless of underlying drivers, then surveillance frameworks calibrated under historical seasonal assumptions risk becoming progressively inadequate as the climate continues to warm. The challenge ahead is not merely documenting winter activity, but establishing operationally feasible, scientifically rigorous, and politically coordinated surveillance systems capable of detecting meaningful biological change against a background of spatial heterogeneity and methodological variation.

5. Conclusion

We provide the first continental-scale evidence, together with a longitudinal temporal analysis, of *Ae. albopictus* egg-laying winter activity, showing that winter monitoring is both feasible and necessary for understanding population ecology in temperate Europe. Photoperiod structures winter activity windows across latitudes, with southern populations maintaining substantial year-round activity. Within-region temporal trends suggest increasing winter activity, though drivers cannot be definitively identified from observational data. The current paradigm of May-October surveillance leaves winter ecology almost entirely unstudied, potentially missing critical dimensions of population persistence, invasion dynamics, and arbovirus risk. Our findings demonstrate that winter activity is not negligible: it is common, structured, variable, and possibly increasing. Future surveillance should expand temporal coverage, particularly in southern Europe, where winter activity is most substantial, and research should prioritise multi-year standardised monitoring to validate and extend these preliminary continental-scale patterns.

6. References

1. Lühken R, Brattig N, Becker N. Introduction of invasive mosquito species into Europe and prospects for arbovirus transmission and vector control in an era of globalization. Infect Dis Poverty. 2023;12:109. https://doi.org/10.1186/s40249-023-01167-z

2. Delrieu M, Martinet J-P, O'Connor O, Viennet E, Menkes C, Burtet-Sarramegna V, et al. Temperature and transmission of chikungunya, dengue, and Zika viruses: A systematic review of experimental studies on Aedes aegypti and Aedes albopictus. Current Research in Parasitology & Vector-Borne Diseases. 2023;4:100139. https://doi.org/10.1016/j.crpvbd.2023.100139

3. Adhami J, Reiter P. Introduction and establishment of Aedes (Stegomyia) albopictus skuse (Diptera: Culicidae) in Albania. J Am Mosq Control Assoc. 1998;14:340–3.

4. European Centre for Disease Prevention and Control. Mosquito maps [Internet]. 2026 [cited 2022 Feb 22]. https://ecdc.europa.eu/en/disease-vectors/surveillance-and-disease-data/mosquito-maps. Accessed 22 Feb 2022

5. Farooq Z, Segelmark L, Rocklöv J, Lillepold K, Sewe MO, Briet OJT, et al. Impact of climate and Aedes albopictus establishment on dengue and chikungunya outbreaks in Europe: a time-to-event analysis. The Lancet Planetary Health. 2025;9:e374–83. https://doi.org/10.1016/S2542-5196(25)00059-2

6. Cattaneo P, Salvador E, Manica M, Barzon L, Castilletti C, Di Gennaro F, et al. Transmission of autochthonous Aedes-borne arboviruses and related public health challenges in Europe 2007–2023: a systematic review and secondary analysis. The Lancet Regional Health - Europe. 2025;51:101231. https://doi.org/10.1016/j.lanepe.2025.101231

7. Pisaneschi G, Manfredi P, Landi A, Stollenwerk N, Aguiar M. When Few Mosquitoes Are Enough: Dengue outbreaks in non-endemic areas. One Health. 2026;22:101308. https://doi.org/10.1016/j.onehlt.2025.101308

8. Tegar S, Brass DP, Purse BV, Cobbold CA, White SM. Temperature-sensitive incubation, transmissibility and risk of *Aedes albopictus* -borne chikungunya virus in Europe. Journal of the Royal Society Interface. 2026;23:20250707. https://doi.org/10.1098/rsif.2025.0707

9. European Centre for Disease Prevention and Control. Seasonal surveillance for chikungunya virus disease in the EU/EEA for 2025 [Internet]. 2025 [cited 2026 Apr 21]. https://www.ecdc.europa.eu/en/chikungunya-virus-disease/surveillance-and-updates/seasonal-surveillance. Accessed 21 Apr 2026

10. Marini G, Manica M, Arnoldi D, Inama E, Rosà R, Rizzoli A. Influence of Temperature on the Life-Cycle Dynamics of Aedes albopictus Population Established at Temperate Latitudes: A Laboratory Experiment. Insects. 2020;11:808. https://doi.org/10.3390/insects11110808

11. Del Lesto I, De Liberato C, Casini R, Magliano A, Ermenegildi A, Romiti F. Is Asian tiger mosquito (*Aedes albopictus*) going to become homodynamic in Southern Europe in the next decades due to climate change? R Soc open sci. 2022;9:220967. https://doi.org/10.1098/rsos.220967

12. Germano KDO, De Souza LAF, Do Amaral AMR, Honório NA, Camara TL, Da Costa-Ribeiro MCV. Embryonic dormancy in Aedes aegypti and Aedes albopictus (Diptera: Culicidae): A survival and dispersal mechanism. Journal of Vector Borne Diseases. 2025;62:253–60. https://doi.org/10.4103/jvbd.jvbd_115_24

13. Denlinger DL, Armbruster PA. Mosquito diapause. Annu Rev Entomol. 2014;59:73–93. https://doi.org/10.1146/annurev-ento-011613-162023

14. Da Re D, Marini G, Bonannella C, Laurini F, Manica M, Anicic N, et al. VectAbundance: a spatio-temporal database of Aedes mosquitoes observations. Sci Data. Nature Publishing Group; 2024;11:636. https://doi.org/10.1038/s41597-024-03482-y

15. Bueno-Mari R, Jiménez-Peydró R. First observations of homodynamic populations of Aedes albopictus (Skuse) in Southwest Europe. Journal of Vector Borne Diseases. 2015;52:175.

16. Lührsen DS, Zavitsanou E, Cerecedo-Iglesias C, Pardo-Araujo M, Palmer JRB, Bartumeus F, et al. Adult Aedes albopictus in winter: implications for mosquito surveillance in southern Europe. The Lancet Planetary Health. 2023;7:e729–31. https://doi.org/10.1016/S2542-5196(23)00170-5

17. Palmer JRB, Oltra A, Collantes F, Delgado JA, Lucientes J, Delacour S, et al. Citizen science provides a reliable and scalable tool to track disease-carrying mosquitoes. Nat Commun. 2017;8:916. https://doi.org/10.1038/s41467-017-00914-9

18. Virgillito C, Longo E, De Marco CM, Serini P, Zucchelli MV, Montarsi F, et al. Involving citizen scientists in monitoring arthropod vectors of human and zoonotic diseases: The case of Mosquito Alert in Italy. Science of The Total Environment. 2024;948:174847. https://doi.org/10.1016/j.scitotenv.2024.174847

19. Di Luca M. Sorveglianza delle zanzare in Italia [Internet]. Roma: Istituto Superiore di Sanità; 2022. https://www.iss.it/-/rapporto-istisan-22/22-sorveglianza-delle-zanzare-in-italia.-a-cura-di-marco-di-luca

20. Muñoz-Sabater J, Dutra E, Agustí-Panareda A, Albergel C, Arduini G, Balsamo G, et al. ERA5-Land: a state-of-the-art global reanalysis dataset for land applications. Earth Syst Sci Data. 2021;13:4349–83. https://doi.org/10.5194/essd-13-4349-2021

21. Hijmans RJ. geosphere: Spherical Trigonometry [Internet]. 2010 [cited 2026 Mar 6]. p. 1.6-5. https://doi.org/10.32614/CRAN.package.geosphere

22. Roiz D, Rosà R, Arnoldi D, Rizzoli A. Effects of Temperature and Rainfall on the Activity and Dynamics of Host-Seeking *Aedes albopictus* Females in Northern Italy. Vector-Borne and Zoonotic Diseases. 2010;10:811–6. https://doi.org/10.1089/vbz.2009.0098

23. Becker N, Petric D, Zgomba M, Boase C, Madon M, Dahl C, et al. Mosquitoes and Their Control. Berlin, Heidelberg: Springer Berlin Heidelberg; 2010.

24. Urbanski J, Mogi M, O'Donnell D, DeCotiis M, Toma T, Armbruster P. Rapid Adaptive Evolution of Photoperiodic Response during Invasion and Range Expansion across a Climatic Gradient. The American Naturalist. 2012;179:490–500. https://doi.org/10.1086/664709

25. Lounibos LP, Escher RL, Nishimura N. Retention and Adaptiveness of Photoperiodic Egg Diapause In Florida Populations of Invasive Aedes albopictus. Journal of the American Mosquito Control Association. 2011;27:433–6. https://doi.org/10.2987/11-6164.1

26. Collantes F, Delgado JA, Alarcón-Elbal PM, Delacour S, Lucientes J. First confirmed outdoor winter reproductive activity of Asian tiger mosquito (Aedes albopictus) in Europe. analesbio [Internet]. 2014 [cited 2026 Mar 31]; https://doi.org/10.6018/analesbio.36.12

27. Haddad N, Omran H, Amraoui F, Zakhia R, Mousson L, Failloux A-B. The tiger mosquito in Lebanon two decades after its introduction: A growing health concern. Churcher TS, editor. PLoS Negl Trop Dis. 2022;16:e0010206. https://doi.org/10.1371/journal.pntd.0010206

780 28. Jia P, Chen X, Chen J, Lu L, Liu Q, Tan X. How does the dengue vector mosquito Aedes
781 albopictus respond to global warming? Parasites Vectors. 2017;10:140.
782 https://doi.org/10.1186/s13071-017-2071-2

783 29. Carrieri M, Albieri A, Angelini P, Baldacchini F, Venturelli C, Zeo SM, et al. Surveillance of
784 the chikungunya vector Aedes albopictus (Skuse) in Emilia-Romagna (northern Italy):
785 organizational and technical aspects of a large scale monitoring system. Journal of Vector
786 Ecology. 2011;36:108–16. https://doi.org/10.1111/j.1948-7134.2011.00147.x

787 30. Erazo D, Pietroiusti R, Ghisbain G, Colón-González FJ, Pironon S, Van Bortel W, et al.
788 Limited evidence for the impact of climate change on the recent range expansion of the malaria
789 vector *Anopheles stephensi* in the Horn of Africa. Environ Res Lett. 2026;21:064028.
790 https://doi.org/10.1088/1748-9326/ae51a7

791 31. Lyberger K, Robinson AR, Couper L, Delwel I, Glidden C, Qian C, et al. A Scoping Review
792 of Mosquito Vector Range Shifts: Widespread Expansions and Evidence Gaps in Climate
793 Attribution. Global Change Biology. 2025;31:e70551. https://doi.org/10.1111/gcb.70551

794 32. Erazo D, Grant L, Ghisbain G, Marini G, Colón-González FJ, Wint W, et al. Contribution of
795 climate change to the spatial expansion of West Nile virus in Europe. Nat Commun. Nature
796 Publishing Group; 2024;15:1196. https://doi.org/10.1038/s41467-024-45290-3

797 33. Hart WS, Hurrell JW, Kaye AR, Chand M, Keeling MJ, Thompson RN. Climate variability
798 amplifies the need for vector-borne disease outbreak preparedness. Proc Natl Acad Sci USA.
799 2025;122:e2507311122. https://doi.org/10.1073/pnas.2507311122

Supplementary Materials

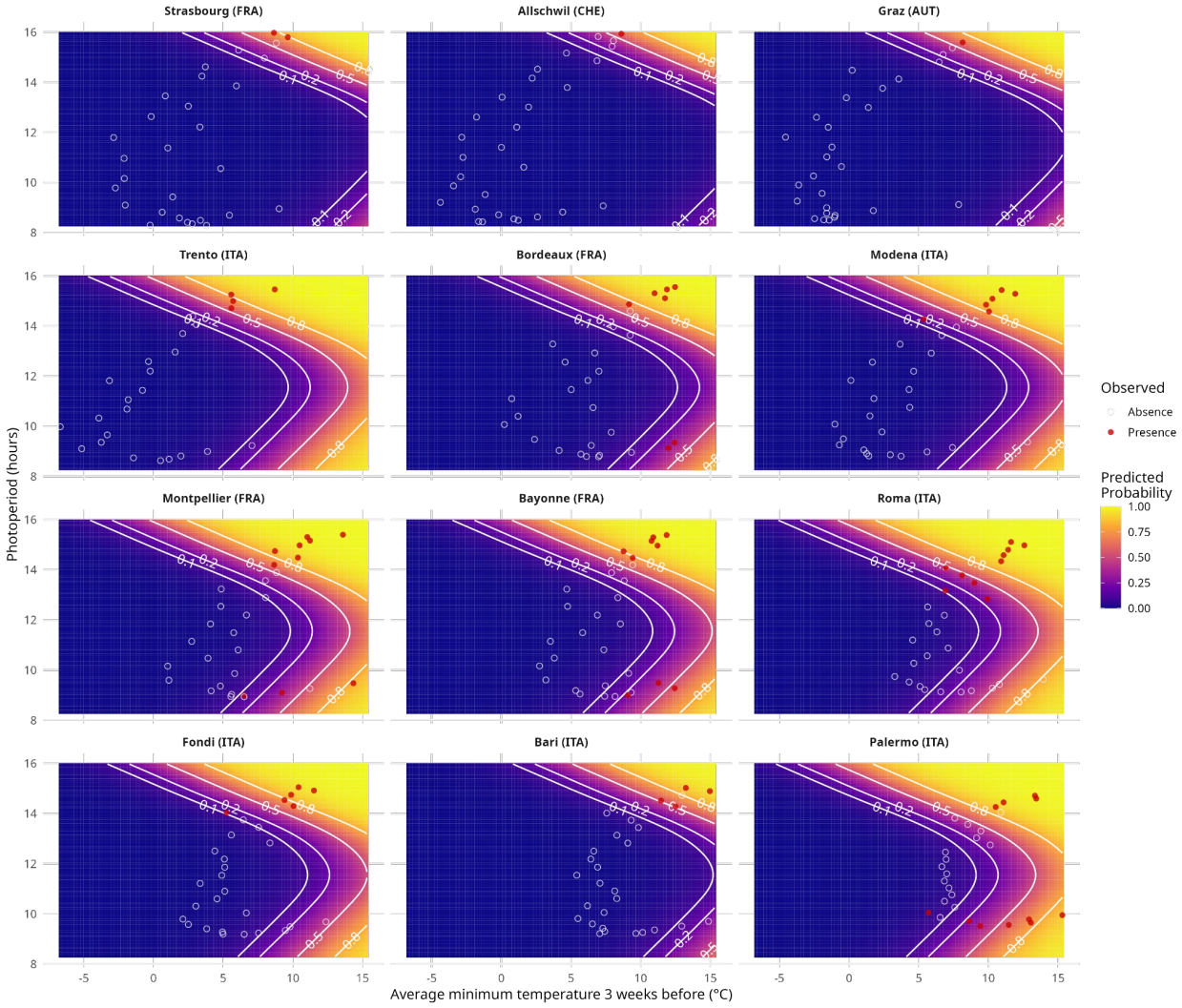

Fig. SM1. Two-dimensional predictions in photoperiod × temperature space (continental analysis) for 12/14 locations (Vienna and Siena were excluded because no positive ovitraps were detected). Marginal effect heatmap with location random effects excluded. White contour lines = 10%, 20%, 50%, 80% probability thresholds. Points = observed presences (filled red) and absences (open white).

Table SM2. Predictive performance metrics for the continental-scale GAM. Overall model performance evaluated using two probability thresholds: default binary threshold (0.5) and Youden's index-optimised threshold (closest to top-left of ROC curve, maximising sensitivity + specificity - 1). Metrics include area under the ROC curve (AUC), accuracy (proportion correctly classified), sensitivity (true positive rate), specificity (true negative rate), precision (positive predictive value), and F1 score (harmonic mean of precision and recall).

Metric	Default 0.5	Optimal top left (0.264)
Accuracy	0.925	0.913
Sensitivity	0.964	0.916
Specificity	0.775	0.901
Precision	0.943	0.973
F1 Score	0.953	0.944
ROC AUC	0.972	0.972

Table SM3. Location-specific predictive performance of the continental winter activity model. Per-location accuracy metrics at Youden-optimised thresholds, ordered by latitude (north to south: Switzerland 47.6°N to Italy 38.1°N). Performance variation reflects differences in positivity prevalence (3% at northern sites vs. 41% at Palermo), sample size (25-30 trap-weeks per location), and local climate variability. Northern locations with minimal activity (Allschwil, Graz: 1 positive observation each) show perfect classification but limited inference. Southern Mediterranean locations (Roma, Palermo) exhibit lower specificity, reflecting higher baseline positivity and complex seasonal dynamics. Model discrimination remains excellent across all locations (AUC range: 0.864-1.000).

Location	Country	n	Positives	Prevalence	Sensitivity	Specificity	Precision	F1 Score	Accuracy	AUC
Allschwil	CHE	30	1	0.033	1.000	1.000	1.000	1.000	1.000	1.000
Graz	AUT	28	1	0.036	1.000	1.000	1.000	1.000	1.000	1.000
Strasbourg	FRA	29	2	0.069	0.963	1.000	1.000	0.981	0.966	1.000
Trento	ITA	25	4	0.160	1.000	1.000	1.000	1.000	1.000	1.000
Modena	ITA	29	6	0.207	0.957	0.833	0.957	0.957	0.931	0.986
Bari	ITA	29	4	0.138	0.960	1.000	1.000	0.980	0.966	0.980
Fondi	ITA	29	6	0.207	1.000	0.833	0.958	0.979	0.966	0.978
Bordeaux	FRA	30	7	0.233	0.957	0.714	0.917	0.936	0.900	0.975
Montpellier	FRA	30	10	0.333	0.900	0.800	0.900	0.900	0.867	0.970
Bayonne	FRA	30	9	0.300	0.952	0.778	0.909	0.930	0.900	0.968
Roma	ITA	29	10	0.345	0.895	0.500	0.773	0.829	0.759	0.895
Palermo	ITA	27	11	0.407	0.938	0.727	0.833	0.882	0.852	0.864

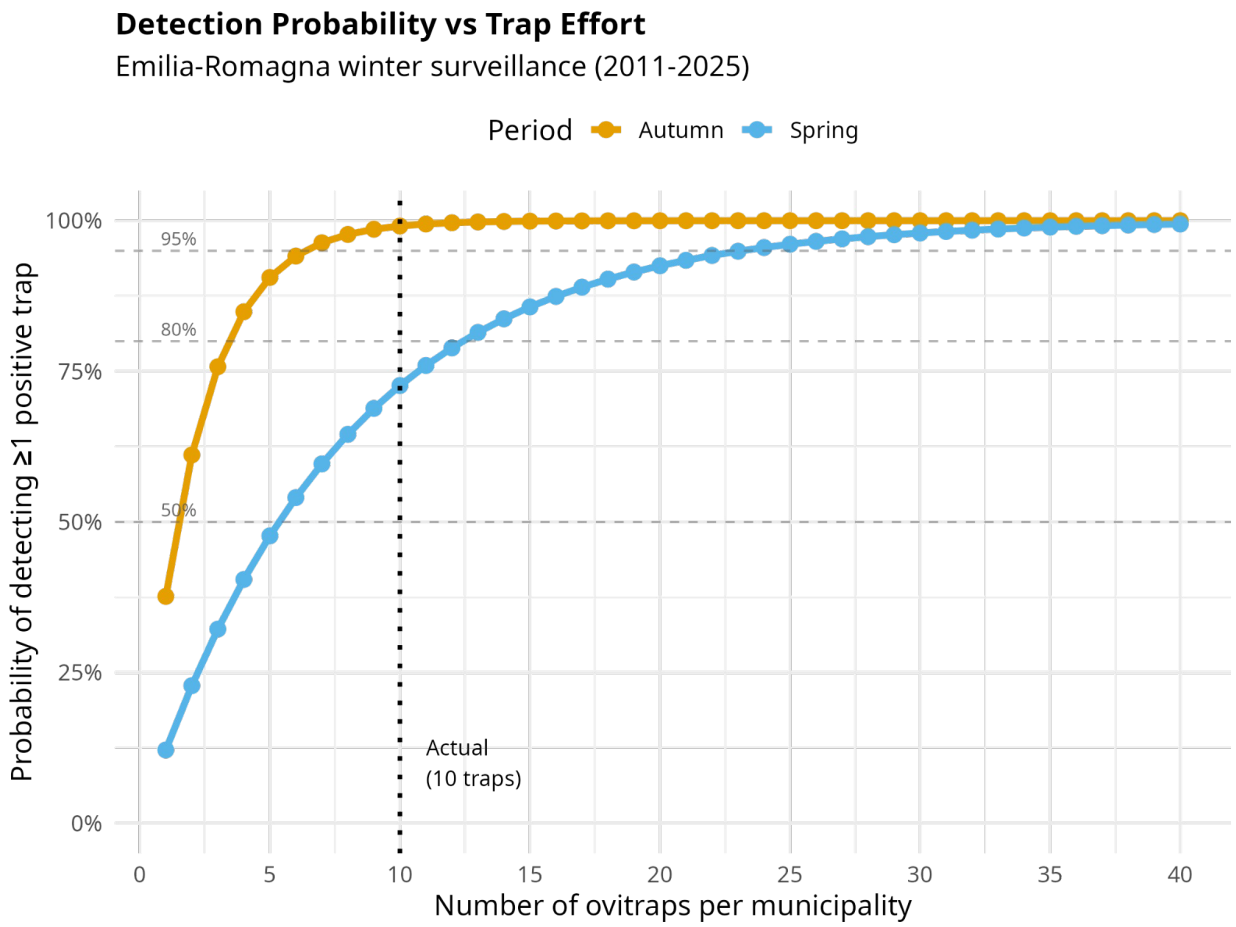

Figure SM4. Trap effort requirements for winter surveillance. Rarefaction curves showing detection probability (probability of detecting ≥1 positive trap) as a function of trap number for autumn (orange) and spring (blue) periods, based on observed mean positivity rates from Emilia-Romagna 2011-2025 (Autumn 37.6%, Spring 12.2%). Horizontal dashed lines indicate detection thresholds: 50% (minimum), 80% (standard surveillance), and 95% (high confidence). The vertical dotted line shows actual deployment (median 10 traps per municipality-week). Autumn surveillance substantially exceeded the 80% threshold (requiring only 4 traps), while spring surveillance fell short (requiring 13 traps), resulting in differential statistical power between periods.